

# DYNAMIC RESPONSE OF SLENDER/THIN REINFORCED PRECAST CONCRETE WALLS USING SHAKING TABLE

Nor Hayati Binti Abdul Hamid<sup>1</sup> and Iwan Surdano<sup>2</sup>

<sup>1</sup>Lecturer, Faculty of Civil Engineering, 40450 UiTM, Shah Alam, Selangor

<sup>2</sup>Project Engineer, Baker Consultant, Washington, New Zealand

## ABSTRACT

Two geometrically identical three-eighths full scale of thin/slender precast wall panels constructed with different base block connections are tested under several earthquake excitations using shaking table. Specimen 1 is designed with a high longitudinal reinforcement ratio with a fixed-base conventional monolithic connection. Specimen 2 is designed with one-half of longitudinal reinforcement ratio Specimen 1 with a rocking-base connection. Both of the walls are designed to carry gravity loading of 34kN and a 50kN supplementary inertia mass is seated on a separate frame at a pin-based connection to represent the initial impulse from earthquake. A shaking table is used to imitate the selected past earthquake records. Specimen 1 is tested under the Taft earthquake excitation with Peak Ground Acceleration (PGA)=0.2g, El Centro (PGA=0.4g) and Kobe (PGA=0.8g), while Specimen 2 undergoes Taft (PGA=0.2g) and El Centro (PGA=0.4g). The dynamic response of Specimen 1 is significantly influenced by its tendency towards permanent out-of-plane deformation. The experimental result shows that Specimen 1 collapsed with a maximum in-plane displacement of 90mm at 5.2 second. Specimen 2 experienced horizontal cracks at bottom one third of the wall. The surface cracks became wider during 0.4g PGA El Centro motion and a large ductility demanded was localised over a very short plastic hinge zone (PHZ). The specimen gradually collapsed due to tensile fracture of the longitudinal starter bars within the grouted zone. This research demonstrates that thin/slender precast wall panel with an excessive longitudinal reinforcement bars is not stable with height to thickness ratio of 60:1 subjected to strong ground shaking. A high ratio of longitudinal reinforcement in walls can generate large in-plane diagonal compressive strut leading to out-of-plane buckling behaviour.

**Keywords:** Displacement Compatibility, Earthquake Excitation, Shaking Table, Shear-buckling, Strut-and-tie Model

## 1.0 INTRODUCTION

Thin/slender precast walls are normally used in the construction of warehouse type buildings. These walls often perform a dual function of providing the exterior cladding as well as resisting loads. The loads may arise from a combination roof (gravity) and out-of-plane wind and/or seismic loadings. In seismic regions, the walls are expected to resist in-plane seismic forces. Figure 1 depicts such a system, where lateral load resisting system is provided by wall panels in both primary directions. Although for this class of building the gravity axial stresses in the walls are not great, the building can nevertheless generate significant seismic force through the roof inertia. These lateral loads must be resisted by certain walls.

For reasons of construction economy and ease of handling, in recent years structural engineers have been trying to increase the wall height while maintaining a constant wall thickness. Walls with height to thickness ratios of 60:1 are not uncommon, with only a single layer reinforcement to provide strength and maintain minimum concrete cover. This is in stark contrast to design codes such as NZS 3101 and ACI 318-99 that require the height to thickness ratios not exceeding 30:1 for seismic design which can resist compression and bending. For example, according to NZS 3101:1995 which provides guidance for non-load bearing wall panels as stated in clause 12.3.2.4 where:

*"Overall thickness of non-load bearing wall panels and enclosure walls shall not less than neither 100mm, nor less than 1/30 the distance between supporting, or enclosing members".*

This clause means that if the wall has a thickness of 100mm, the height between supports should not exceed 3m and for 150mm thickness, the maximum height of the wall can only be 4.5m. But the limitation of wall thickness can be waived as long as rational analysis using basic engineering principles supported by experimental works stated in Clause 12.3.2.4:

*"Limits of the thickness .....required by 12.3.2 may be waived where, instead of the empirical rules of 12.3.6, rational analysis or test results show adequate strength and stability at the ultimate limit state."*

If the slenderness ratio is exceeding 30, a rational analysis should be performed as long as it is accepted by engineers and designers. The experimental results together with principles of engineering must be used to show that the walls are stable, resistance against compression and bending under serviceability limit state.

Given the well defined code limitations as mentioned above, it appears somewhat surprising that designers take the liberty to exceed the standard slenderness ratio (30:1) by significant margins without conducting proof-of-concept tests. Moreover, there appears to be no straight forward textbook analysis that a designer could conduct to confirm the stability and general safety of the wall. Thus, this paper presents an experimental study on two thin walls with height to thickness ratio of 60:1. Precast systems with grouted connections were utilised to provide a monolithic connection between the wall and foundation. Experimental results from the dynamic shaking table testing and some relevant information on quasi-

static from previous study will be used to analyse and predict the dynamic response of thin/slender walls.

## 2.0 FINDINGS FROM PREVIOUS RESEARCH

A lot of research had been conducted on precast wall panels under reverse quasi-static cyclic loading. Most of these precast wall panels were connected to foundation beam using fixed-base connection to emulate the structural behaviour under current code of practice. The wall-foundation interface connection plays an important role in seismic behaviour of the wall under severe/extreme ground shaking. The formation of plastic hinge zone (PHZ) at this interface will cause cracking, spalling and crushing of concrete. Furthermore, the structural damage on thin/slender precast walls becomes crucial when lateral buckling and stability are the main issues.

To address this problem, [1] tested five precast walls with 4/10-scale under in-plane seismic loading. These walls had slenderness ratio of 50:1 together with variation of width and amount of longitudinal reinforcement bars. The results revealed that the walls with higher ratio of longitudinal reinforcement failed by shear-buckling mechanism at the base of the wall panel, while those walls with low longitudinal reinforcement ratio failed due to tensile bar fracture and spalling of concrete cover at bottom of the wall.

Further investigation was carry out [2] by using four slender precast walls with variations of axial loading and length of lap-splices. The walls were designed with a slenderness ratio and longitudinal reinforcement ratio of 75:1 and 1.72%, respectively. Even though out-of-plane buckling occurs at mid-height of the wall but his study also showed that the flexural performance can be improved by using welded lap splices between wall-foundation interfaces. He also demonstrated that slender walls could perform better with starter bars clustered at edges of the wall as compare to those walls with uniform spacing of the longitudinal reinforcement through the entire length of the wall.

In order to validate the experimental work performed [1,2], a global computational model which can predict the possible failure mechanism of reinforced concrete wall was further investigated [3]. He modelled these failure mechanism using displacement compatibility and force-equilibrium in the form of strut-and-tie model. He proposed that the seismic behaviour between shear-buckling and shear-flexure can be predicted using displacement compatibility. Moreover, out-of-plane failure mechanism for both global elastic buckling and local inelastic buckling can be modelled as force-equilibrium in strut-and-tie model. The analytical model developed [3] showed a good agreement with McMenamin's and Chiewanichakorn's experimental results. Yet, [3] recommended that more experimental works on thin wall panels should be carried out in order to validate his out-of-plane buckling model due to global elastic buckling. Hence, this study is partly addressing this concern.

The current code of NZ 3101:1995 should be reviewed to accommodate the demand of end-user community and life-safety requirements. Thus, [4] studied the seismic performance of two half-scaled precast concrete walls tested under reversed quasi-static static regime to meet the demand. The first wall was designed according to requirements of the New Zealand Concrete Structures Standard (NZS 3101) with a fixed-based monolithic

emulation precast concrete wall, while the second wall designed with a rocking-base connection. Both walls had a height to thickness ratio of 30:1 and reinforcement ratios of 0.84% and 0.25% in the longitudinal and transverse direction, respectively. The wall connection was designed to emulate the behaviour of the cast-in-place connection where plasticity was restricted at the base of the wall. An innovative connection was used to join the wall to the foundation beam. The wall was embedded in a recess prepared inside the foundation beam. The gap left between the wall and the foundation beam then was filled with the shrinkage compensating grout. This method was proposed to overcome the difficulties in a precast construction, whereby the connection are often joined by overlapped bars to form continuity. The first wall performed as a ductile cast-in-place unit with a degradation of strength observed when it reached 2.5% drift. But the second wall performed better than the first wall. No damage was observed in the second wall with rocking base connection because the wall-foundation interface was protected against the impact.

Up to date, only a limited experimental works were conducted on precast wall panels subjected to earthquake excitation using shaking table. Consequently, the following section will focus on the experimental study of walls under selected earthquake excitation.

## 3.0 EXPERIMENTAL STUDY ON THE DYNAMIC PERFORMANCE OF THIN WALL PANELS

Two identical geometries of precast concrete walls with a height to thickness ratio of 60:1 were tested under earthquake excitation on the shaking table at the University of Canterbury. Laboratory height restrictions limited the model scale to 3/8 of the prototype dimensions. The specific scale was chosen mainly due to the available reinforcing bars. The model, strength and ductility were determined based on the idealised prototype warehouse buildings as shown in Figure 1. It is expected that W1 to W4 in north-south direction is the most heavily loaded laterally in-plane direction. The prototype walls have a fixed base, while their top are pinned and restrained against out-of-plane translation due to a presence of a roof truss system.

Figure 2 depicts the reinforcement layout for both walls. The dimension of each wall is 2.81m height, 0.9m wide and 47mm thick. Other design parameters for prototype, Specimens 1 and 2 are shown in Table 1. The concrete compressive strength was  $f'_c = 30$  MPa, and 6mm Grade 300 deformed bars with measured yield strength of  $f_y = 350$  MPa were used for the longitudinal and

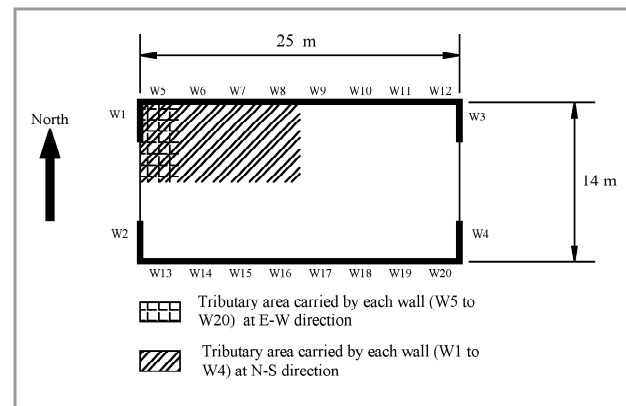


Figure 1: Idealised plan view of a typical warehouse building

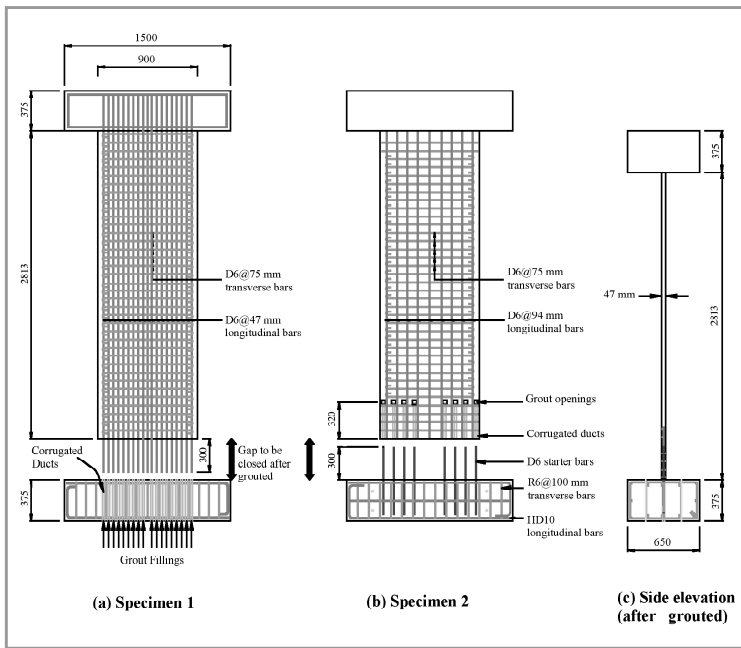


Figure 2: Reinforcement layout for Specimens 1 and 2

Table 1: Design parameters for Prototype, Specimens 1 and 2

Properties	Unit	Prototype	Specimen 1	Specimen 2
<b>Dimensions</b>				
Height ( $H$ )	mm	7500	2813	2813
Width ( $B$ )	mm	2400	900	900
Thickness ( $t$ )	mm	125	47	47
Aspect ratio ( $t/H$ )		1/60	1/60	1/60
Inertial Load	kN	464	95	95
Gravity Load ( $P = W_y$ )	kN	114	17	17
<b>Reinforcement</b>				
Bar diameter ( $d_b$ )	mm	16	6	6
Yield strength ( $f_y$ )	MPa	NA	350	350
$\rho_{transverse}$		0.81%	0.81%	0.81%
$\rho_{longitudinal}$		1.27%; 0.54%	1.27%	0.54%
<b>Concrete compression strength (<math>f'_c</math>)</b>				
7 days	MPa	NA	25	30
28 days ( $f'_c$ )	MPa	NA	35	38
Beginning of testing	MPa	NA	42	44
<b>Grout compression strength</b>				
7 days	MPa	NA	29	31
28 days ( $f'_c$ )	MPa	NA	42	44
Beginning of testing	MPa	NA	45	48

transverse reinforcement. The foundation beams were designed to remain elastic and to prevent any plastic deformation propagating from the panels. HD10 and R6 reinforcement bars were utilised for the longitudinal and transverse reinforcement bars for foundation beams, respectively.

Both of specimens were constructed on a "strong back" steel casting bed and foundation beam attached to these specimens using extruded bars. Strong back is used to ensure that the walls could be easily lifted and tilted into the final position (shaking table) without inducing any damage. The strong back was also employed during grouting process which enables the mortar to be placed in a vertical position. Subsequently, this experimental work is replicating how it is conducted on site. Accordingly, the constructions of these specimens, experimental set-up together with testing procedures are presented in the following section.

### 3.1 CONSTRUCTION OF SPECIMENS 1 AND 2

The main objective for this research is to investigate whether buckling failure is likely to occur when a thin wall has a high longitudinal reinforcement ratio. Figure 3 shows the

construction process of both specimens to be examined. Figure 3(a) shows the photographic picture of the steel strong back used for casting of specimens. Both walls were cast together with the top gravity block forming a monolithic connection. An additional block was also cast to provide gravitational stress similitude and placed on the top of the gravity block.

A photographic record of reinforcement layout of Specimens 1 and 2 are presented in Figures 3(b) and (d), respectively. Specimen 2 differed from the Specimen 1 in two ways. Firstly, Specimen 2 had one-half of the longitudinal reinforcement less than in Specimen 1 and secondly, the corrugated ducts were placed over the lower 300 mm of the wall as shown in Figure 2(b). Starter bars protruding from the foundation beam were grouted into the wall. Figure 3(c) shows the ducted grouted connection that was used to join the wall specimen to the foundation base block. The grouted ducts were inserted inside the base block with each duct opening being 3.5 times the bar diameter. The longitudinal reinforcing bars from the wall were inserted 300 mm into the ducts to give an anchorage of  $50 d_b$  for the development length.

### 3.2 EXPERIMENTAL SETUP AND TESTING PROCEDURES

Figure 4(a) shows the experimental setup for a slender/thin wall anchored to the shaking table via the foundation beam. A pair of guide beams, each with two roller bearings, was positioned on both sides of the top gravity block to provide lateral stability to that block. This fixing allowed the top block to move freely within the in-plane direction but prevent any lateral (out-of-plane) displacement at the top of the block. Figure 4(b) shows the side elevation of Specimen 1 with concrete block located on top of the wall. A 50 kN supplementary inertia mass was seated on a separate frame at a pin-based connection to represent impulse from earthquake excitation. A photographic

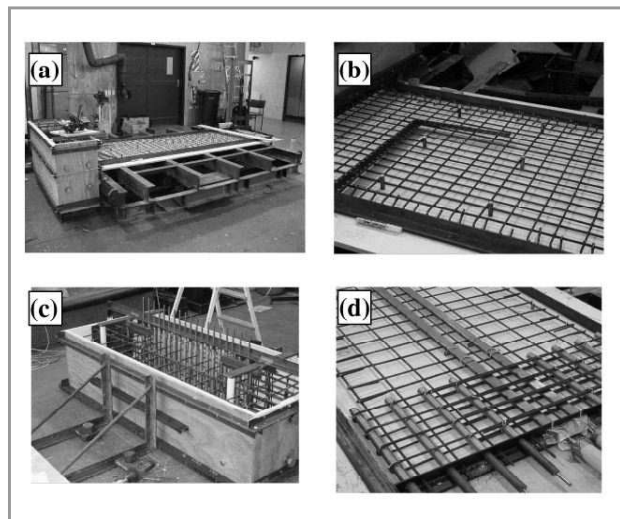
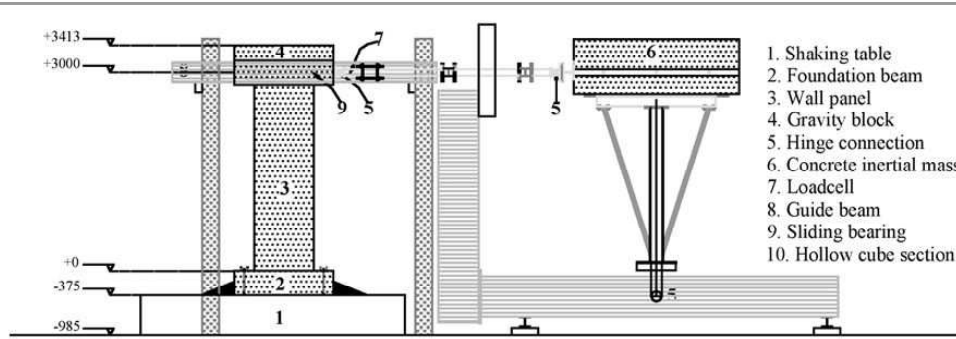


Figure 3: Construction process of Specimen 1 and 2 ; (a) 'strong back' steel casting bed used for both specimens; (b) Specimen 1; reinforcement layout; (c) Specimen 1; grout connection base; and (d) Specimen 2; reinforcement layout.

view of the complete setup is shown in Figure 4(c). Figure 4(d) shows the location of the instrumentation devices used during the experiments. These mainly consisted of linear potentiometers to measure displacement in both out-of-plane and in-plane directions; and accelerometers to measure in-plane and out-of-plane acceleration response. Out-of-plane displacement was measured at two vertical lines along the height of the specimens. Six potentiometers were installed to measure the in-plane displacement at the top block and along the height

of the specimen wall. Accelerometers were attached to measure the acceleration at particular points: on the shaking table, the top block, the inertial block and the mid height of the wall specimen for the out-of-plane acceleration.

The present shaking table at University of Canterbury testing laboratory is driven by input from the displacement record. All of the input acceleration records needed to be double integrated to provide displacement records that can be used as the input excitation driver for the table motion. This shaking



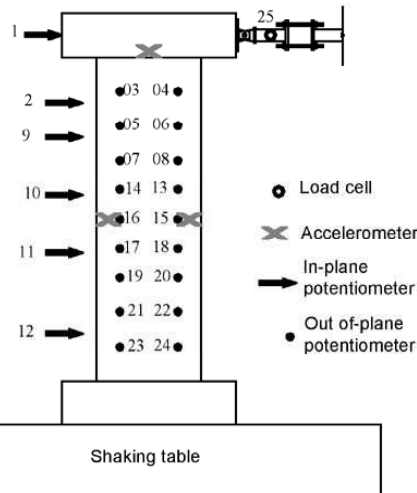
a) Elevation of test setup



(b) Side elevation of slender wall



(c) Photographic view of experimental setup



(d) Instrumentation layout for dynamic testing

Figure 4: The experimental set-up and instrumentation of Specimens 1 and 2

table is a single axis machine with a stroke of  $\pm 120$  mm and a payload capacity of 20 tonne. Within the limitation of the shaking table stroke, some acceleration records which contain low frequency contents require some pre-filtering of the records prior to be used as input excitation. Both low-pass ( $< 0.1$  Hz) and high-pass ( $> 16$  Hz) bandwidth were applied to all of the acceleration records fed to the shaking table; the latter being used to remove certain spurious table frequencies.

A complete chronology order of the dynamic testing on these specimens is tabulated in Table 2. Prior to, and following each earthquake record test, "white-noise" tests were conducted

Table 2: Excitation earthquake records

SPECIMEN 1			
NO	ACCELERATION RECORD	PGA (g)	CODE
01	White Noise	0.05	WN0501
02	Taft	0.20	TAFT201
03	White Noise	0.05	WN0502
04	El Centro	0.40	ELC401
05	White Noise	0.05	WN0503
06	Kobe	0.80	KOBE801

SPECIMEN 2			
NO	ACCELERATION RECORD	PGA (g)	CODE
01	White Noise	0.05	WN0505
02	Taft	0.20	TAFT203
03	White Noise	0.05	WN0506
04	El Centro	0.40	ELC402

to obtain frequency domain inferences of damping and natural frequencies of the specimens. Tracking the changes in the frequencies and damping between main earthquake runs gives an impression of the degree of damage inflicted on the wall due to the previous earthquake motions. The white-noise motion was developed using a random function to acquire acceleration records which have approximately the same power spectral density over wide frequency range. The maximum peak table acceleration for the white-noise tests was set to 0.05g.

Earthquake excitation commenced with 1952 Taft excitation input with PGA scaled to 0.2g. This is considered representative to a moderate level earthquake excitation. Next, the 1940 El Centro N-S acceleration record scaled to produce a PGA of 0.4g was applied as representative of a "design basis" earthquake in a zone of moderate to high seismic risk. Finally, the 1995 Kobe N-S acceleration record with PGA scaled to 0.8g was used to investigate the near-field effects on a high risk seismic zone.

## 4.0 EXPERIMENTAL RESULTS

### 4.1 SPECIMEN 1

The seismic performance of Specimen 1 was significantly influenced by its tendency towards permanent out-of-plane deformation and lateral torsional buckling. The first earthquake ground motion (Taft with PGA=0.2g) led to a reasonably high level of buckling as shown in Figure 5(a) where a significant level out-of-plane deformation can be observed. A maximum out-of-plane displacement of 19 mm was recorded during this excitation. A number of horizontal crack lines were also developed on the surface of wall as shown in Figure 5(b). The cracks mostly formed at the bottom one-third of the wall at the north face and around the top half for the wall's south face.

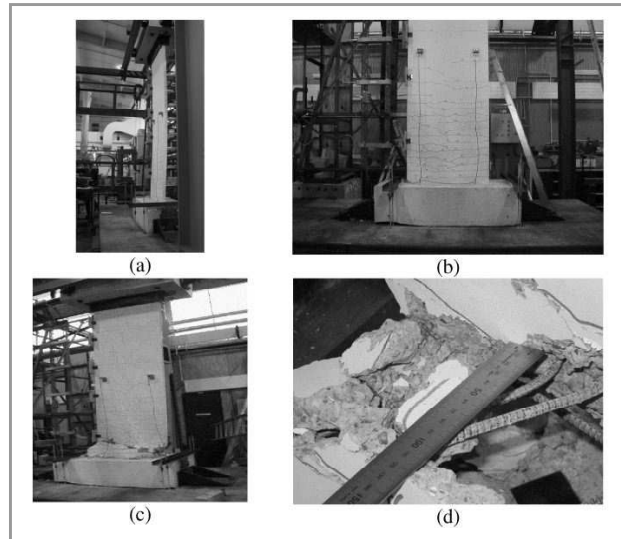


Figure 5: Damages visual observation on Specimen 1; (a) End View of out-of-plane following Taft excitation (PGA=0.2g) deformation; (b) Elevation view of crack pattern on north-face; (c) Out-of-plane buckling shear failure at the end of testing; and (d) Buckled failure zone at the end of testing

Most of the cracks occurred parallel to the horizontal reinforcement. Position of the cracks proved that the specimen bent in a double-curvature mechanism.

Afterward, Specimen 1 was tested under higher amplitude of earthquake excitation. The 1940 El Centro N-S record scaled with PGA =0.4g was applied and further damage occurred with cracks starting to propagate along the diagonal lines. Eventually, Specimen 1 was collapsed during the 1995 Kobe (PGA=0.8g) excitation, due to out-of-plane flexure-shear buckling mechanism near the base of the wall. The full collapsed Specimen 1 at the end of testing is demonstrated in Figures 5(c) and (d).

The transient response of Specimen 1 to the Taft motion is presented in Figure 6. Taft excitation input acceleration record was scaled to a PGA of 0.2g as shown in Figure 6(a). A maximum relative displacement of 27 mm was recorded at the top base block as shown in Figure 6(b) which is equivalent to a drift of 0.9% and a ductility factor of 2.4. Figure 6(c) shows the out-of-plane displacement wall which was gradually translated towards the south-face of the wall in a global buckling sense. Figure 6(d) shows the acceleration at top block vs. in-plane relative displacement.

Figure 7 presents the results of the N-S 1940 El Centro earthquake acceleration record with PGA scaled to 0.4g [Figure 7(a)]. Further damage was induced in the specimen, with the level of out-of-plane deformation increasing from 27 to 52 mm [Figure 7(c)]. This level of displacement is more than one wall thickness, at the mid-height of the wall. A maximum in-plane relative displacement of 49 mm was recorded [Figure 7(b)] which approximately equals to a drift of 1.6% and a ductility level of 4.3. Larger in-plane relative displacement was recorded at 40mm as shown in Figure 7(d).

Figure 8(a) shows the 1995 Kobe input ground motion scaled to a PGA of 0.8g. This level of excitation induced excessive in and out-of-plane deformation leading to complete collapse of the specimen at 5.2 seconds into the earthquake. Collapse occurred when the in-plane displacement reached

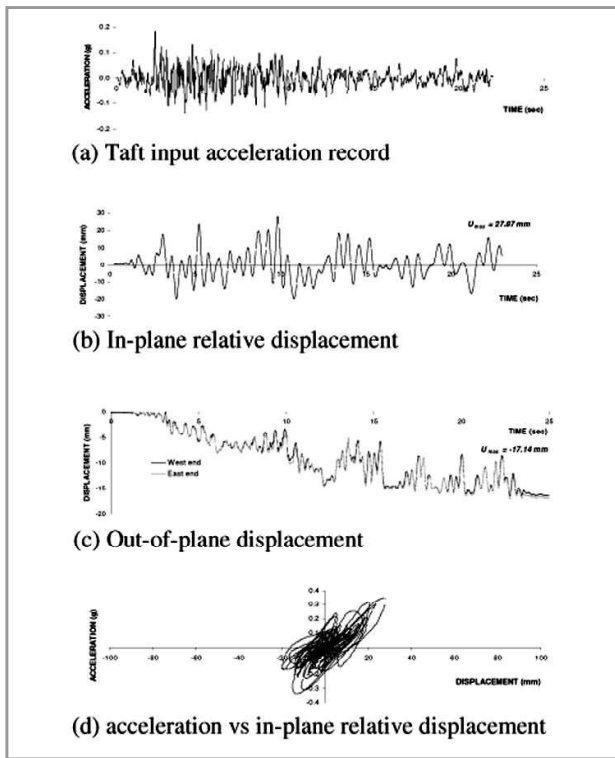


Figure 6: Seismic response of Specimen 1 to Taft excitation with PGA = 0.2g

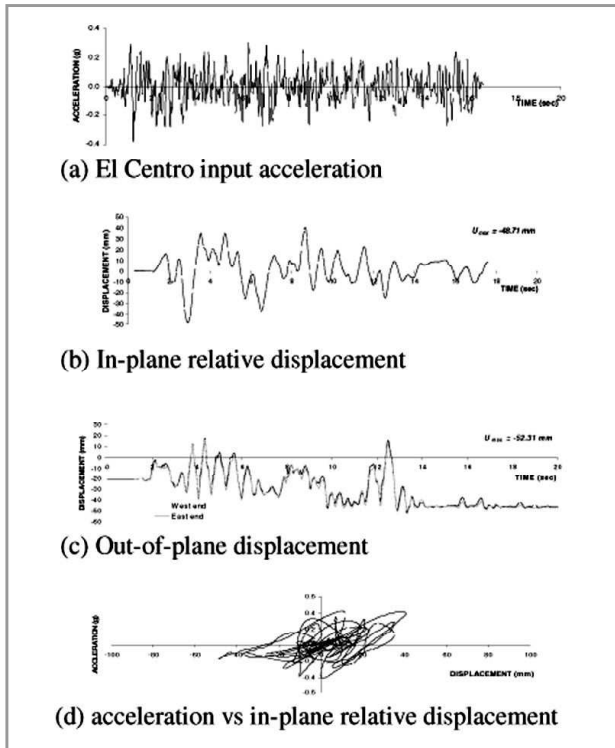


Figure 7: Seismic response of Specimen 1 to El Centro excitation with PGA=0.4g

approximately 90 mm or 3% drift ( $m \approx 8$ ), (refer to Figure 8(b)). When examining Figure 8(c) it is evident that a lateral torsional buckling response occurred slightly before the wall buckled. When the time is 4.7 seconds, the east side of the wall

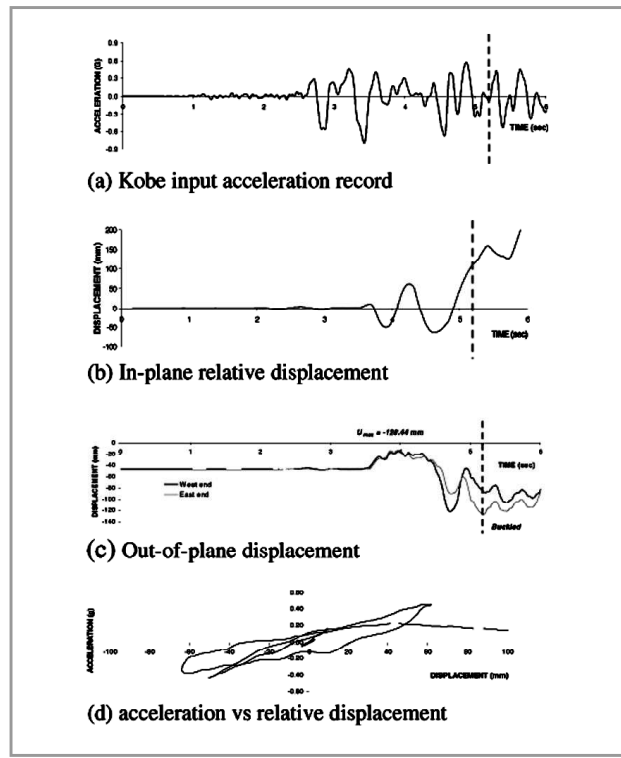


Figure 8: Seismic response of Specimen 1 to Kobe excitation with PGA = 0.8g

experienced a larger out-of-plane displacement compared to the western side of the wall. But during the next reversed cycle (positive relative displacement) at 5.2 seconds peak, due to some tension straightening at the west end, the out-of-plane displacement was reduced while the east counterpart worsened due to the presence of the large compression strut. Figure 8(d) presents the collapse of the walls after the Kobe earthquake excitation was imposed to the wall.

#### 4.2 SPECIMEN 2

Figure 9 presents the photographic experimental results for Specimen 2. Although Specimen 1 experienced significant permanent out-of-plane deformations during only a moderate 0.2g PGA excitation, such behaviour was not observed for Specimen 2. In fact permanent out-of-plane deformation was barely discernable as shown in Figure 9(a). Similar horizontal crack patterns were observed at bottom one third of the wall [Figure 9(b)]. There is one exception that should be noted here. This concerns a network of vertical cracks that occurred in the middle of the wall at the location where a pair of prestressing ducts (for the rocking connection) were placed.

One line of horizontal cracks started to open right at the surface connection between the panel and the base block during the 0.2g Taft excitation. This crack caused rocking like behaviour during the earthquake motion excitation. The surface crack widened during the 0.4g PGA El Centro motion and a large ductility demand was localised over a very short plastic hinge zone. The specimen eventually collapsed due to tensile fracture of the longitudinal starter bars within the grouted duct zone as shown in Figure 9(c). No further spreading of the flexural cracks above the rupture line were observed as shown Figure 9(d).

Figure 10(a) presents the experimental results for the Taft input acceleration record scaled to a PGA of 0.2g. A maximum relative displacement of 21 mm (0.7% drift,  $m = 1.6$ ) as shown in Figure 10(b) was recorded. A maximum of 6 mm out-of-plane deformation was recorded, but looking at the permanent out-of-plane deformation it was shifted from the negative residual (towards north face) to the positive residual (see Figure 9(c)). It is apparent that the out-of-plane deformation for Specimen 2 did not worsen in the same direction following the 0.2g PGA Taft excitation. From acceleration Vs displacement graph (Figure 10(d)), a small level of energy was calculated with an equivalent viscous damping of 0.76%. It can be done by transferring the response into frequency domain and utilising half power bandwidth method.

Figure 11 shows the seismic response of Specimen 2 scaled to the 0.4g PGA El Centro excitation. Figure 11(a) depicts El Centro input acceleration record scaled to a PGA of 0.4g. The acceleration Vs displacement graphs [Figure 11(d)] shows that the west-end reinforcing bar fracture at PGA=0.25g with +45mm in-plane relative displacement. Figure 11(b) shows that the tensile bar fracture at 3.5 seconds. It is contended that at this point the first longitudinal bar fracture occurred due to the excessive strain demand on the very short plastic hinge zone. It is apparent that the bar splicing method is one of the determining factors for the failure mechanism. Prior to failure at  $t = 6.8$  seconds, the out-of-plane displacement was restricted to  $\pm 4$  mm [Figure 11(c)]. This out-of-plane displacement did finally increase to some 9 mm, but this is considered to be an artefact of the in-plane failure. Figure 11(d) also shows a general plot of out-of-plane displacements. Although the maximum out-of-plane displacement occurred during the Taft 0.2g PGA test, this is believed to be induced by the in-plane vibration, but this was not a permanent damage as evidenced

by the small residual out-of-plane displacement which was less than 2 mm.

This investigation of slender/thin walls on shaking table will give some pictures and prediction of damage that will occur during a real earthquake. Even though Malaysia is not in high seismic

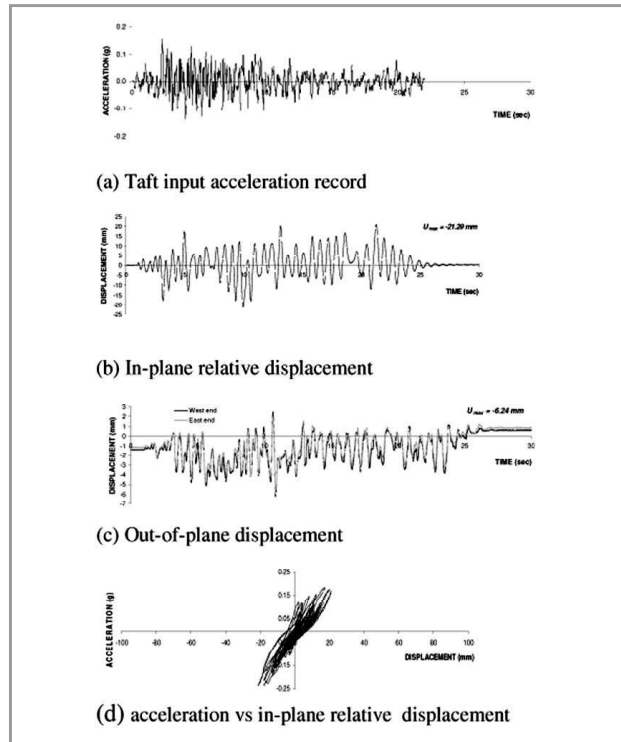


Figure 10: Seismic response of Specimen 2 to Taft excitation with PGA = 0.2g

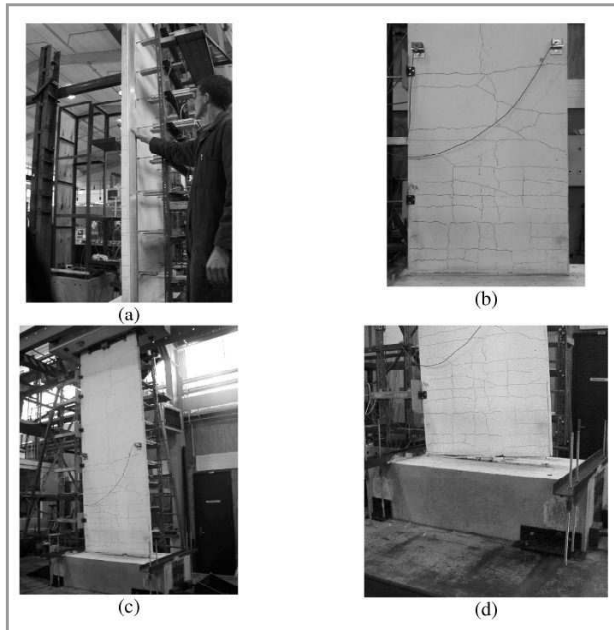


Figure 9: Damage visual observation on Specimen 2: (a) Negligible level of out-of-plane deformation following Taft excitation (PGA = 0.2g); (b) Horizontal crack patterns at bottom one-third of the wall following Taft excitation (PGA=0.2g); (c) Side elevation view at the end of testing after El Centro excitation (PGA = 0.4g); and (d) Close-up view of base at end of testing showing rupture

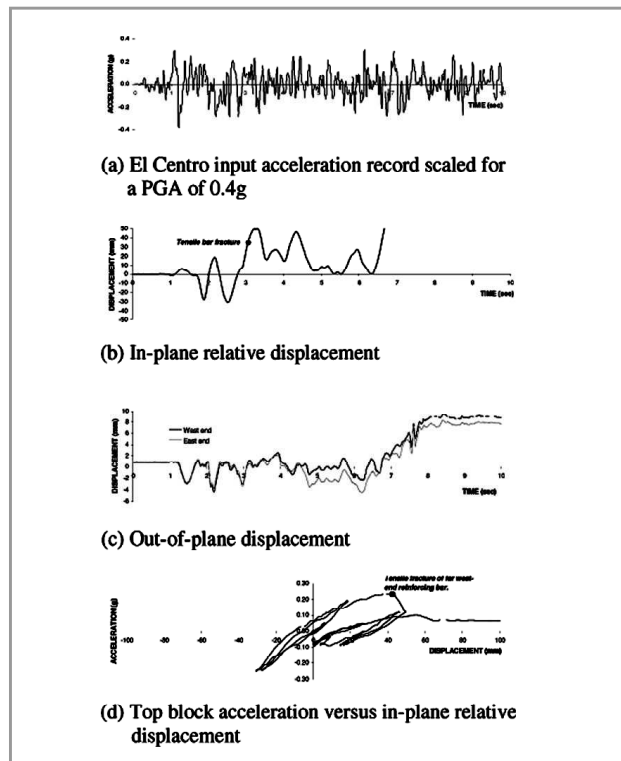


Figure 11: Seismic response of Specimen 2 to El Centro

regions but some amplification factor could be applied to predict on long distant earthquake excitation on a singly reinforced precast wall panel. Since Malaysia's code of practice followed British Standard which do not have any provision of seismic design, it is ideal to review and change the code by implementing Eurocode by 2010. Thus, the experimental work and theoretical analysis should be conducted based on Malaysia environment so that it will suit to our own need not just duplicate from other countries code.

## 5.0 CONCLUSION AND RECOMMENDATIONS

The following conclusions and recommendation are drawn from this study:

1. Although the prescriptive provisions of present design codes (NZS 3101 and ACI 318) limited the height to thickness ratio to 30:1, this research has demonstrated that by providing excessive longitudinal reinforcement also did not stabilise the wall at slenderness ratio of 60:1 and unfortunately the failed by out-of-plane buckling.
2. High ratios of longitudinal reinforcement can generate large in-plane compressive strut-and-tie forces. The in-plane compressive strut forces led to out-of-plane buckling. It is recommended to include the slenderness ratio, amount of reinforcement bars and compressive forces in Euler-based buckling theory which will be presented in next paper.
3. The experimental results revealed that Specimen 1 (fixed-based connection) has severe damage as compared to Specimen 2 (rocking base-connection). A thin/slender precast wall panels become unstable leading to global instability under dynamic testing. Specimen 1 failed by out-of-plane buckling in longitudinal reinforcement bars together with shear failure at wall-foundation interface (plastic hinge zone). The fracture of outermost tension longitudinal reinforcement bars effects the stability of the walls during rocking mechanism in Specimen 2. It is suggested that thin/slender precast wall can be post-tensioned at the centre of walls and any distribution of reinforcement closed to the bottom corner of the wall should be avoided. ■

- [4] Holden, T. J., Restrepo, J. I., Mander, J. B. (2001). A Comparison of Seismic Performance of Precast Concrete Wall Construction: Emulation and Hybrid Approaches, Research Report 2001-4 Department of Civil Engineering, University of Canterbury.

---

## REFERENCES

- [1] McMenamin, A. P. (1999) The Performance of Slender Precast reinforced Cantilever Walls with Roof Level Lateral Displacement Restrain under Simulated In-Plane Seismic Loading, M.E. Thesis, Department of Civil Engineering, University of Canterbury.
- [2] Chiewanichakorn, M. (1999). Stability of Thin Precast Concret Wall Panels Subejected to Gravity and Seismic Forces, M.E. Thesis, Department of Civil Engineering, University of Canterbury.
- [3] Lander, M. R. E. (2001). Analytical Modelling of Reinforced Concrete Wall Behaviour under Seismic Loading, ME Report, Department of Civil Engineering, University of Canterbury.